Title
GERMANIUM BLOCKED IMPURITY BAND (BIB) DETECTORS

Authors
Haller, E.E.
Bauiann, H.
Beeman, J.

Publication Date
1989-02-01

Lawrence Berkeley Laboratory
UNIVERSITY OF CALIFORNIA

Engineering Division

Presented at the IR Detector Technology Workshop,
Mountain View, CA, February 7–9, 1989

Germanium Blocked Impurity Band (BIB) Detectors

E.E. Haller, H. Baumann, J. Beeman, W.L. Hansen, P.N. Luke,
M. Lutz, C.S. Rossington, and I.C. Wu

February 1989

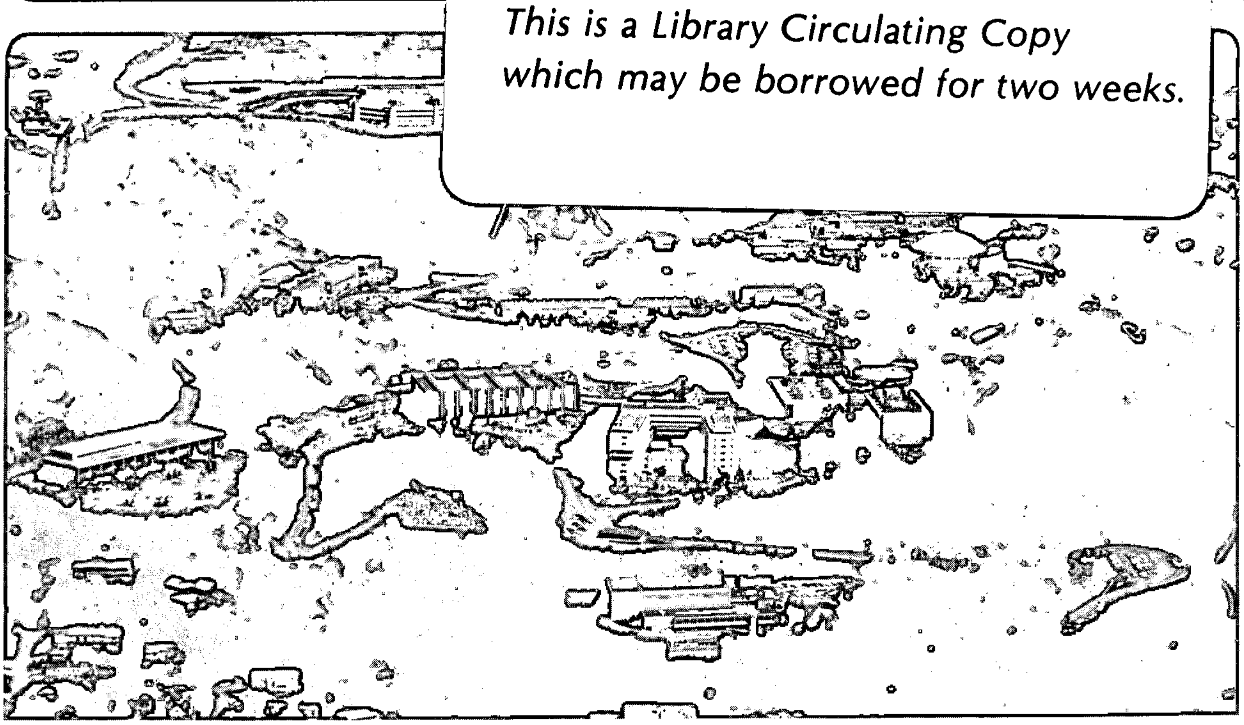

Prepared for the U.S. Department of Energy under Contract Number DE-AC03-76SF00098

DISCLAIMER

LBL-26814

Germanium Blocked Impurity Band (BIB) Detectors

E. E. Haller[1,2], H. Baumann[1,2], J. Beeman[2], W. L. Hansen[2], P. N. Luke[2], M. Lutz[1,2], C. S. Rossington[1,2,3], I. C. Wu[1,2]

Presented at the IR Detector Technology Workshop, February 7-9, 1989, NASA Ames Research Center

[1]University of California at Berkeley

[2]Engineering Division, Lawrence Berkeley Laboratory, 1 Cyclotron Road, Berkeley, CA 94720

[3]Present address: Hewlett-Packard, Opto-Electronic Division, 350 W. Trimble Rd., San Jose, CA 95131

CONTENTS

ACKNOWLEDGMENT

This work was supported by NASA Contract W-14,606X under an interagency agreement with the U.S. Department of Energy under Contract No. DE-AC03-76SF00098.

1. INTRODUCTION

- Extrinsic, photoconductive semiconductor detectors cover the infrared spectrum from a few μm up to 250 μm.

- Photoconductors exhibit high responsivity and low noise equivalent power.

- The Si blocked impurity band (BIB) detector invented by M. D. Petroff and M. G. Stapelbroek has a number of advantages over standard bulk photoconductors. These include:

  - smaller detection volume leading to a reduction of cosmic ray interference

  - extended wavelength response because of dopant wavefunction overlap

  - photoconductive gain of unity

2. Ge BIB

- The success of Si BIB detectors has been a strong incentive for the development of Ge BIB detectors.

- The advantages of Si BIB detectors stated above should, in principle, be realizable for Ge BIB detectors.

- If Ge BIB detectors can be made to work out to 250 μm with high responsivity and sufficiently low dark current, they could replace stressed Ge:Ga photoconductors.

- Can the dark current be reduced to acceptable levels?

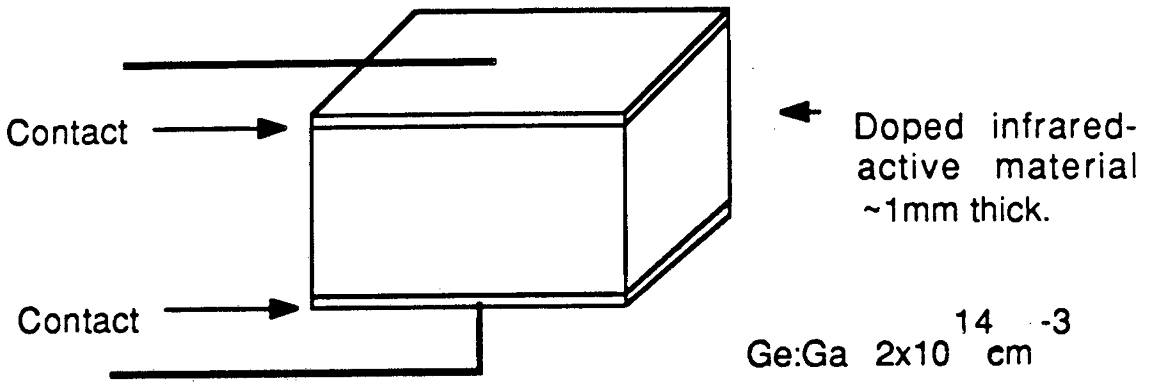

Figure 1(a). Schematic of conventional detector.

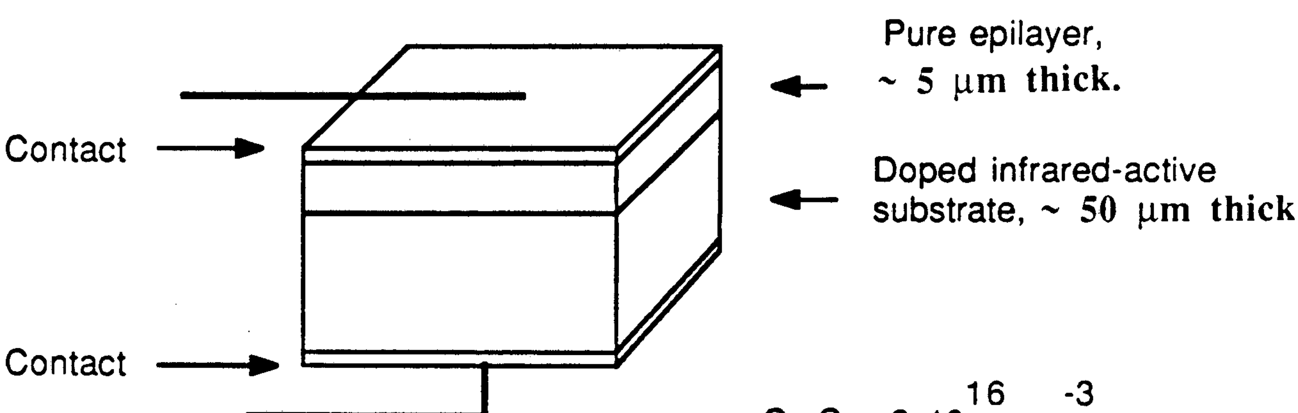

Figure 1(b). Schematic of BIB detector.

XBL 884-1137

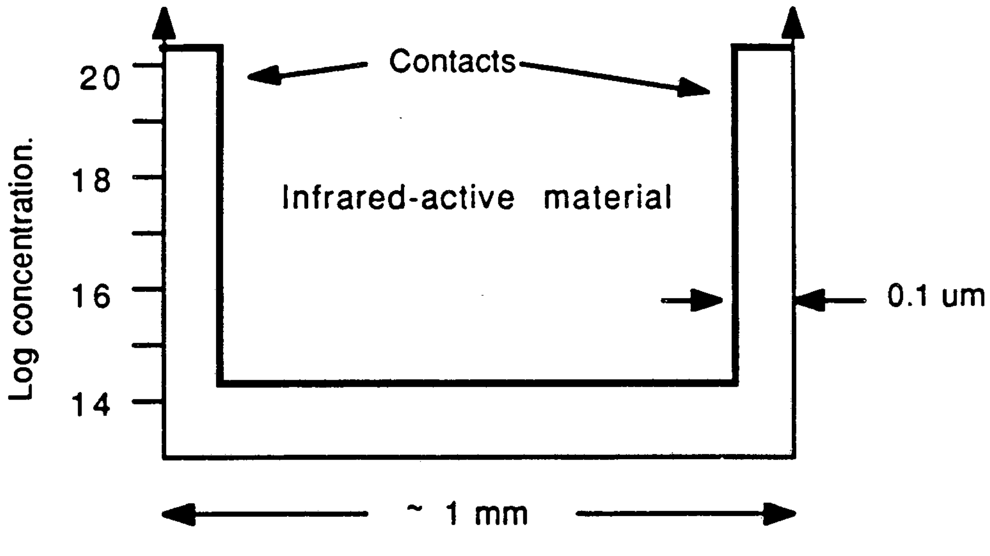

Figure 2(a). Doping levels in a conventional Ge detector.

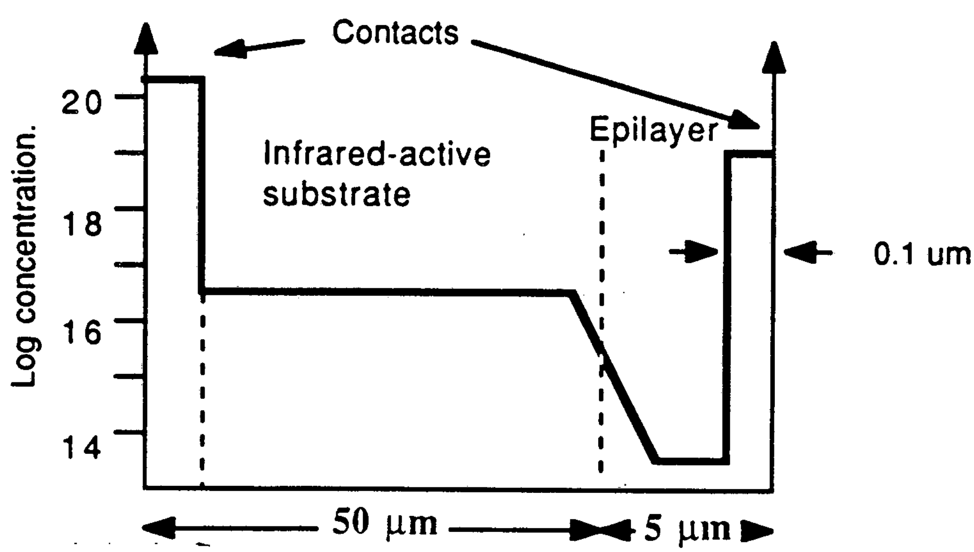

Figure 2 (b). Doping levels in a Ge BIB detector.

XBL 884-1138

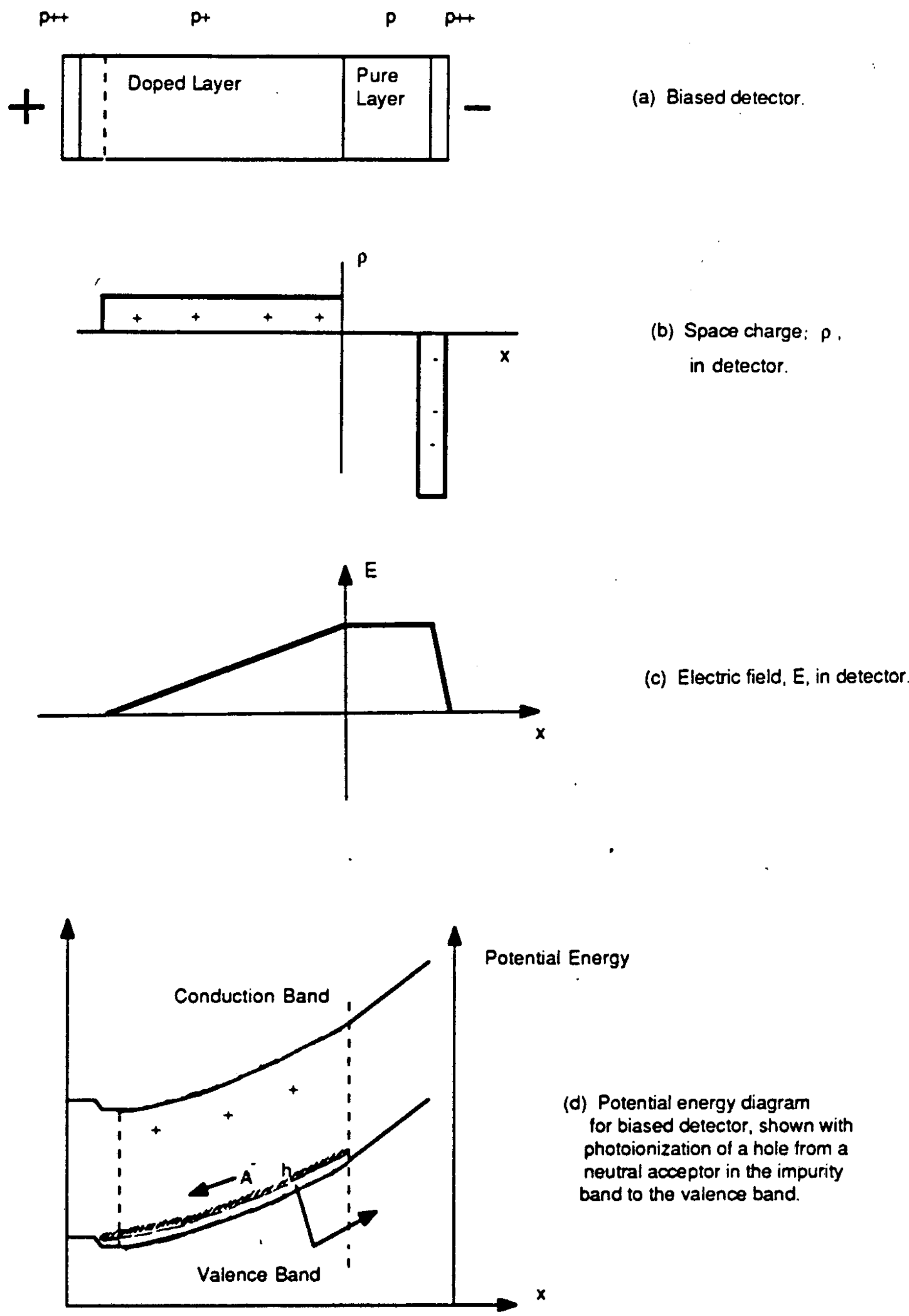

Fig. 3. Schematics of space charge, electric field and potential energy for a reverse biased p-type BIB detector.

XBL 884-1141

3. Ge BIB DETECTOR DEVELOPMENT

3.1. Epitaxial Blocking Layer Devices

3.1.1. Ge epitaxy

- Whereas Si epitaxy techniques have been developed to a very high degree of perfection, Ge epitaxy has been attempted only on a few occasions.

- Ge chemistry is very different from Si chemistry.

- Ultra-pure Ge compounds [$Ge(CH_3)_4$, $Ge(C_2H_5)_4$] are being developed for III-V semiconductor technology. They may be useful to Ge epitaxy.

Substrate choice and preparation

- **We have used a number of different crystals with various crystallographic orientations in the development of Ge epitaxy:**
  - **n-type wafers (~10^{11} cm^{-3}) are used for the electrical characterization of the epitaxial layers which are typically p-type because of residual copper contamination (junction isolation).**
  - **p-type wafers (~10^{15} cm^{-3}) are used for I-V comparison tests with conventional photoconductors.**
  - **p-type wafers (~2×10^{16} cm^{-3}, low compensation) are used for Ge BIB detectors.**

- **Wafer polishing process:**
  - mechanical planar lapping with alumina slurry.
  - mechano-chemical polishing with syton containing H_2O_2.
  - brief etch in HNO_3:HF (3:1) followed by soak in HF (1% in H_2O) to remove oxides.

- **Epitaxy:**
  - first experiments with atmospheric pressure vapor phase epitaxy (VPE). Disadvantage: high substrate temperature, H_2 diluted feed gas (contamination, diffusion of dopants into the blocking layer).
  - current experiments are performed with low pressure VPE. Advantage: low substrate temperature.

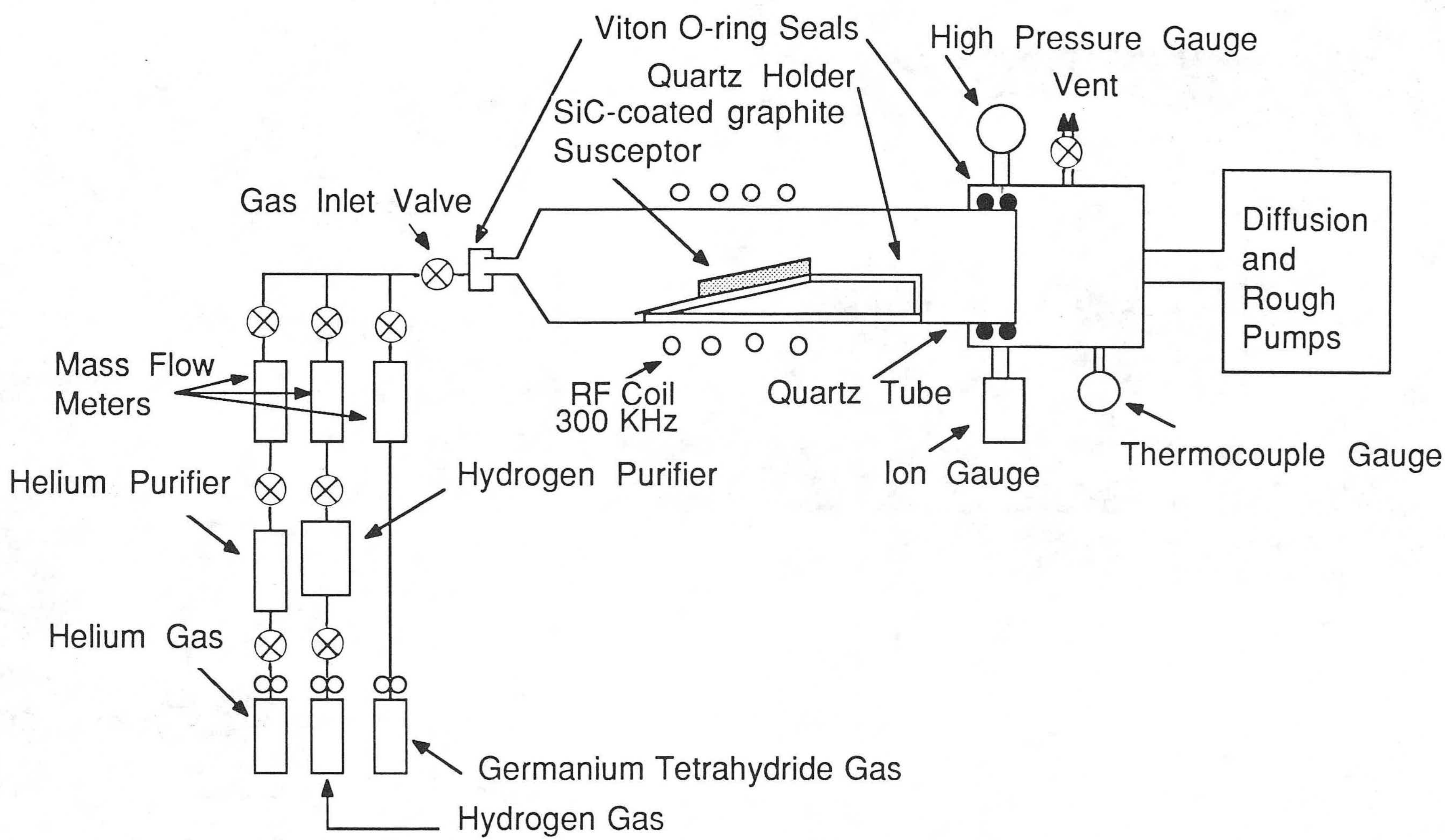

XBL 884-1189

Fig. 4. Schematic of horizontal VPE apparatus. Quartz tube is 5.7 cm O.D. x 75 cm long.

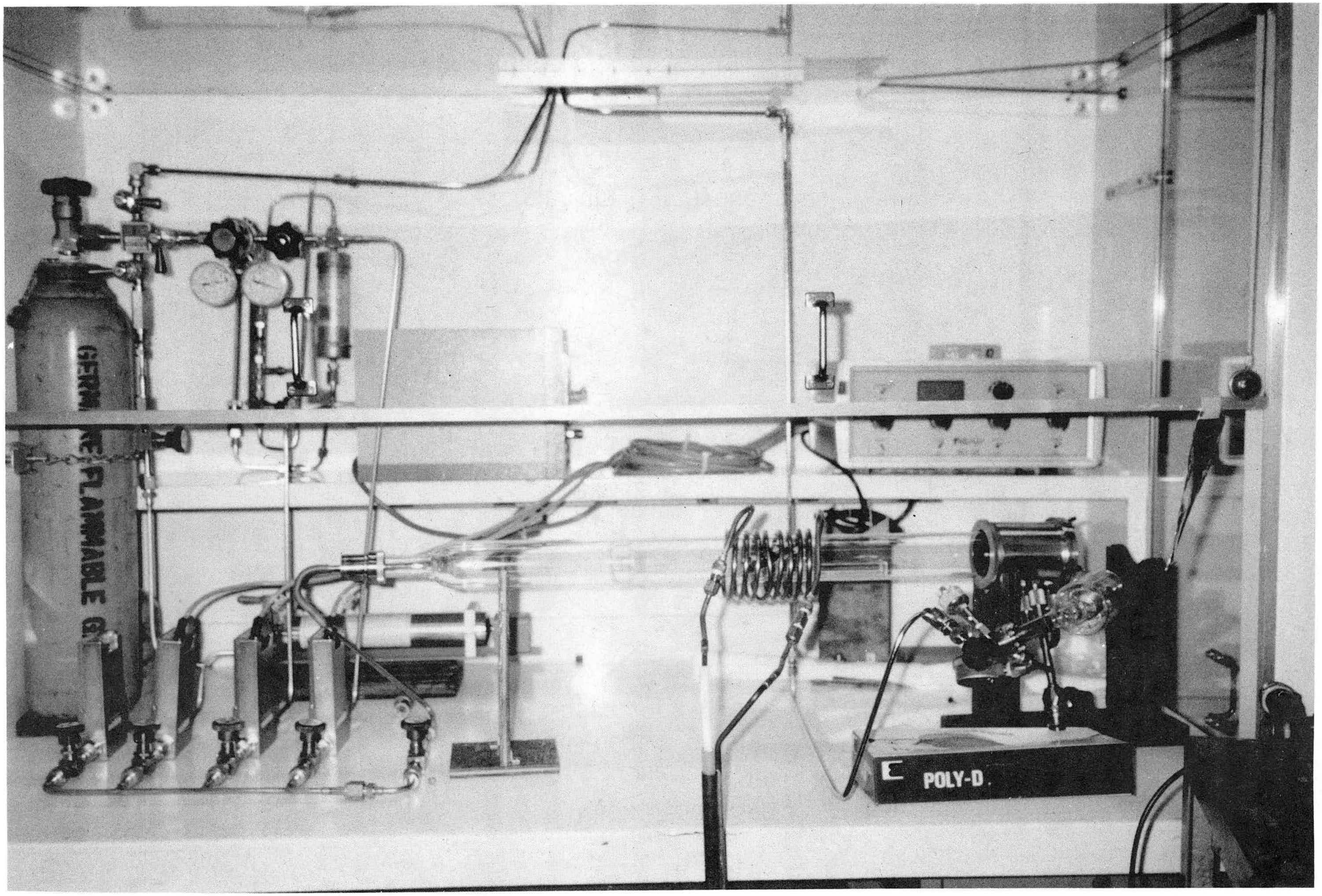

CBB 879-7254

Fig. 5. Photograph of the horizontal VPE chamber.

3.1.2. Characterization of epi layers

- Optical micrographs

- Variable temperature Hall effect and resistivity

- Rutherford backscattering (channeling) spectrometry (RBS)

- Secondary ion spectrometry (SIMS)

- Spreading resistance measurements

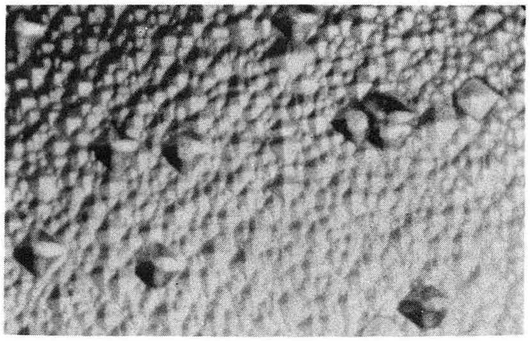

0.03 mm

(100) $N_D - N_A = 1 \times 10^{14} / cm^3$
580 °C; 5 sccm GeH_4,
with H_2 reduction step,
polycrystalline deposition

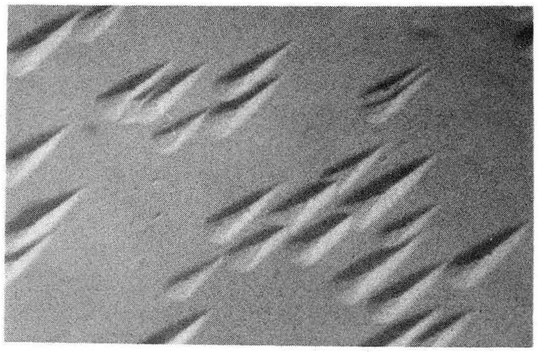

0.03 mm

(113) $N_D - N_A = 2 \times 10^{14} / cm^3$
580 °C; 5sccm GeH_4,
with H_2 reduction step,
no growth (etching)

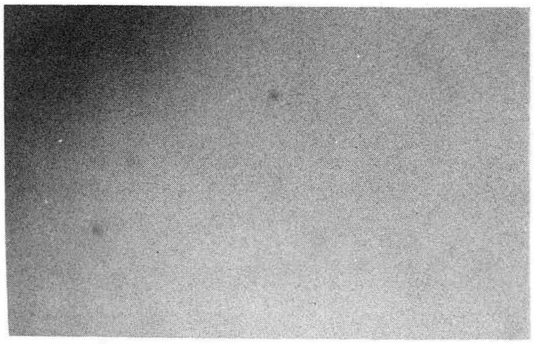

0.03 mm

(113) $N_D - N_A = 5 \times 10^{11} / cm^3$
550 °C; 10sccm GeH_4,
no H_2 reduction step,
single crystal deposition

XBB 892-612

Fig. 6. Optical micrographs of Ge epi layers.

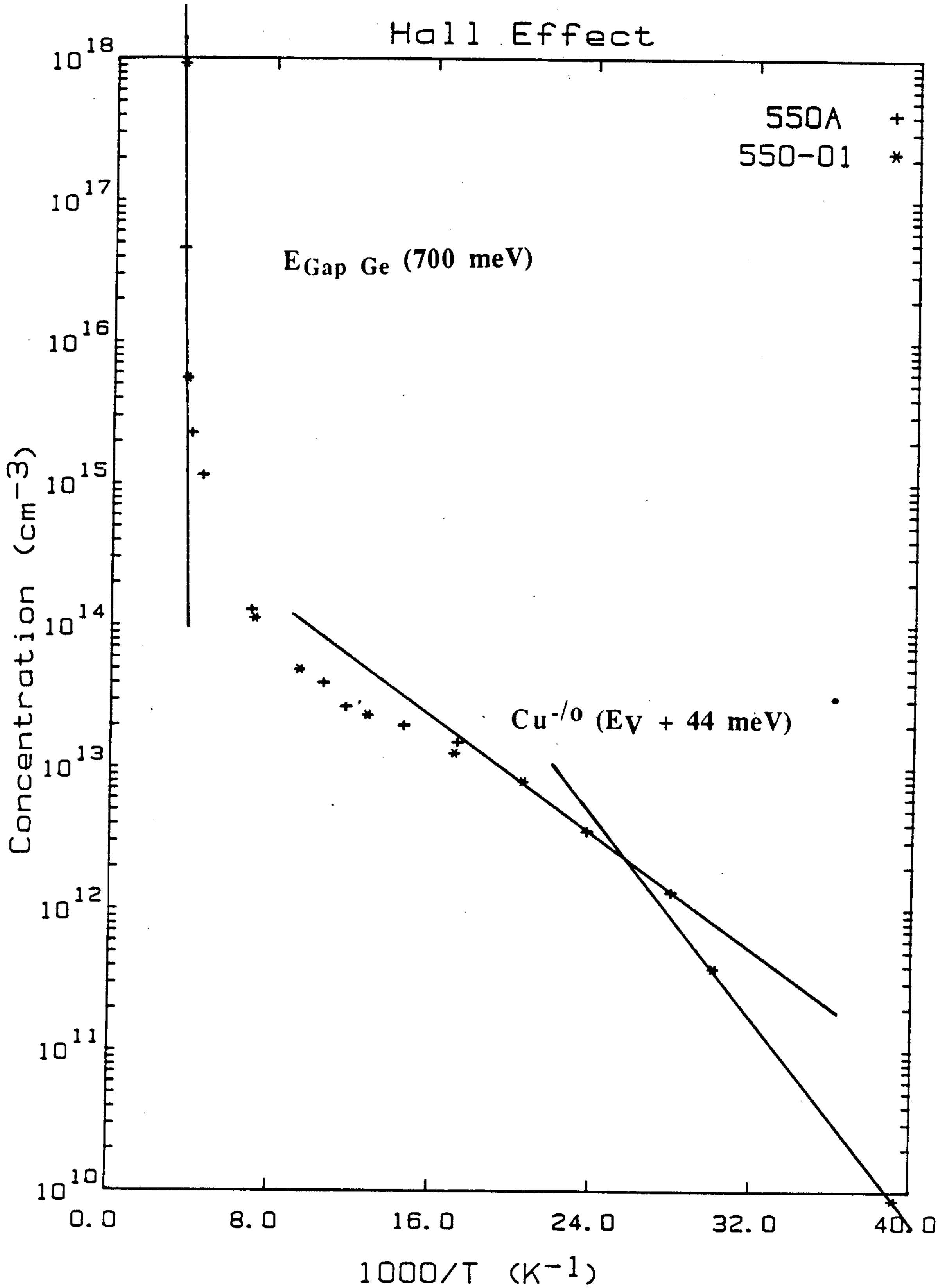

Fig. 7. **Variable temperature Hall effect measurements of a Ge epilayer on an n-type [113] substrate. The hole freeze-out curves indicate a light copper contamination. The two curves (+, $*$) are measurements of the same sample and demonstrate reproducibility.**

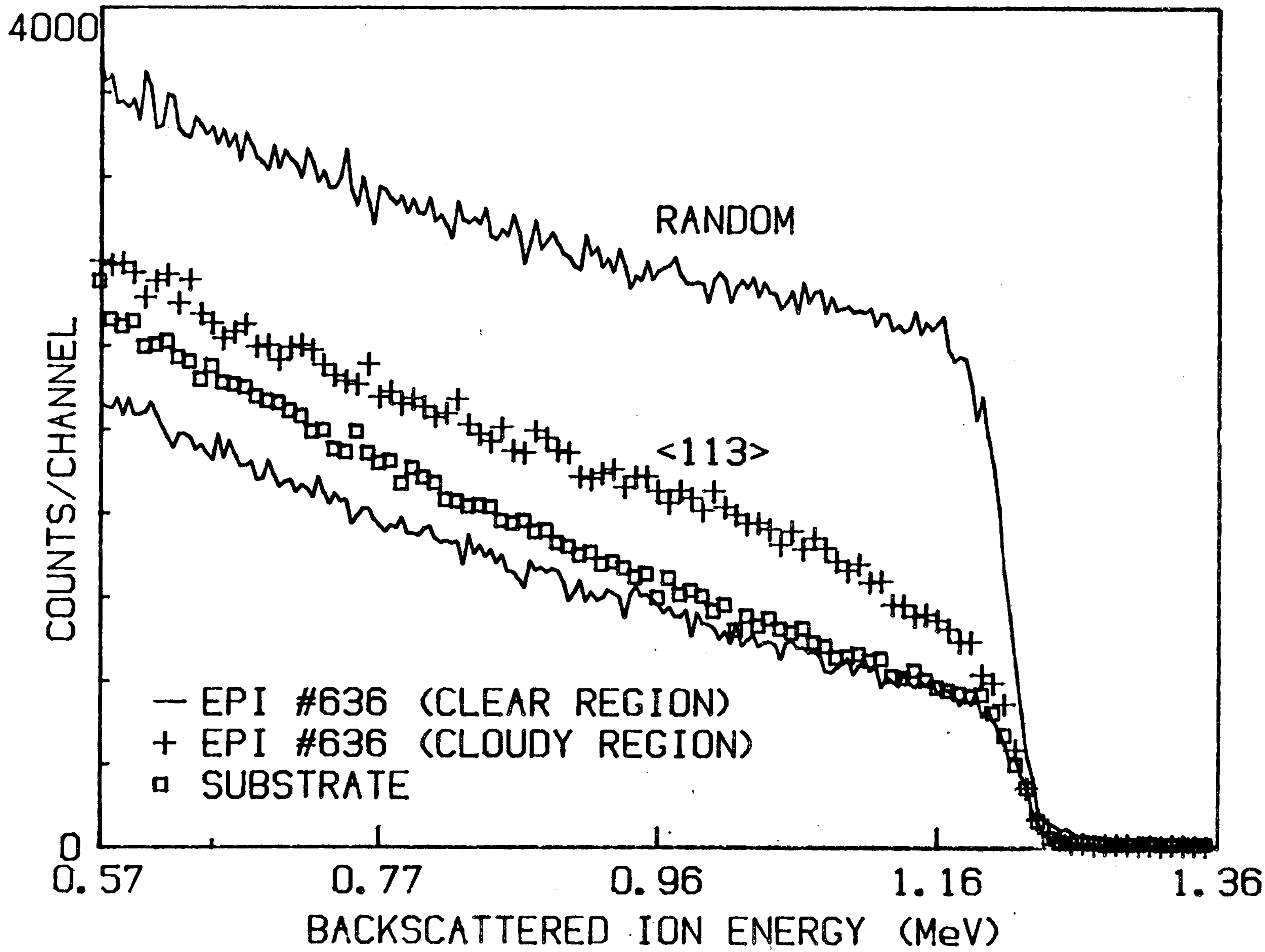

Fig. 8. RBS channeling spectra of a Ge epi film (#636). The "cloudy" region shows significant dechanneling indicating a high defect concentration.

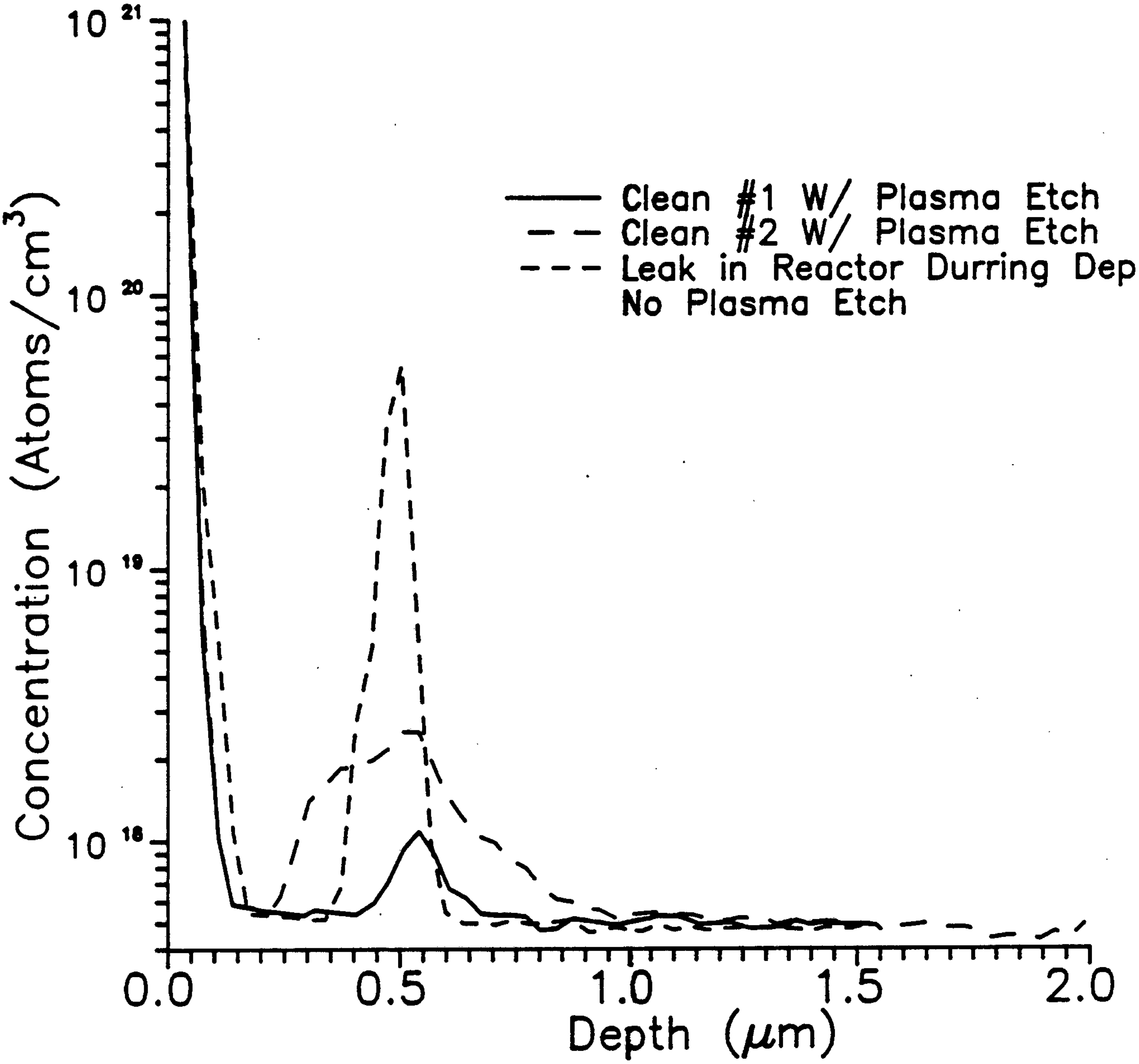

Fig. 9. SIMS of LPVPE Epi Films: Oxygen Concentration

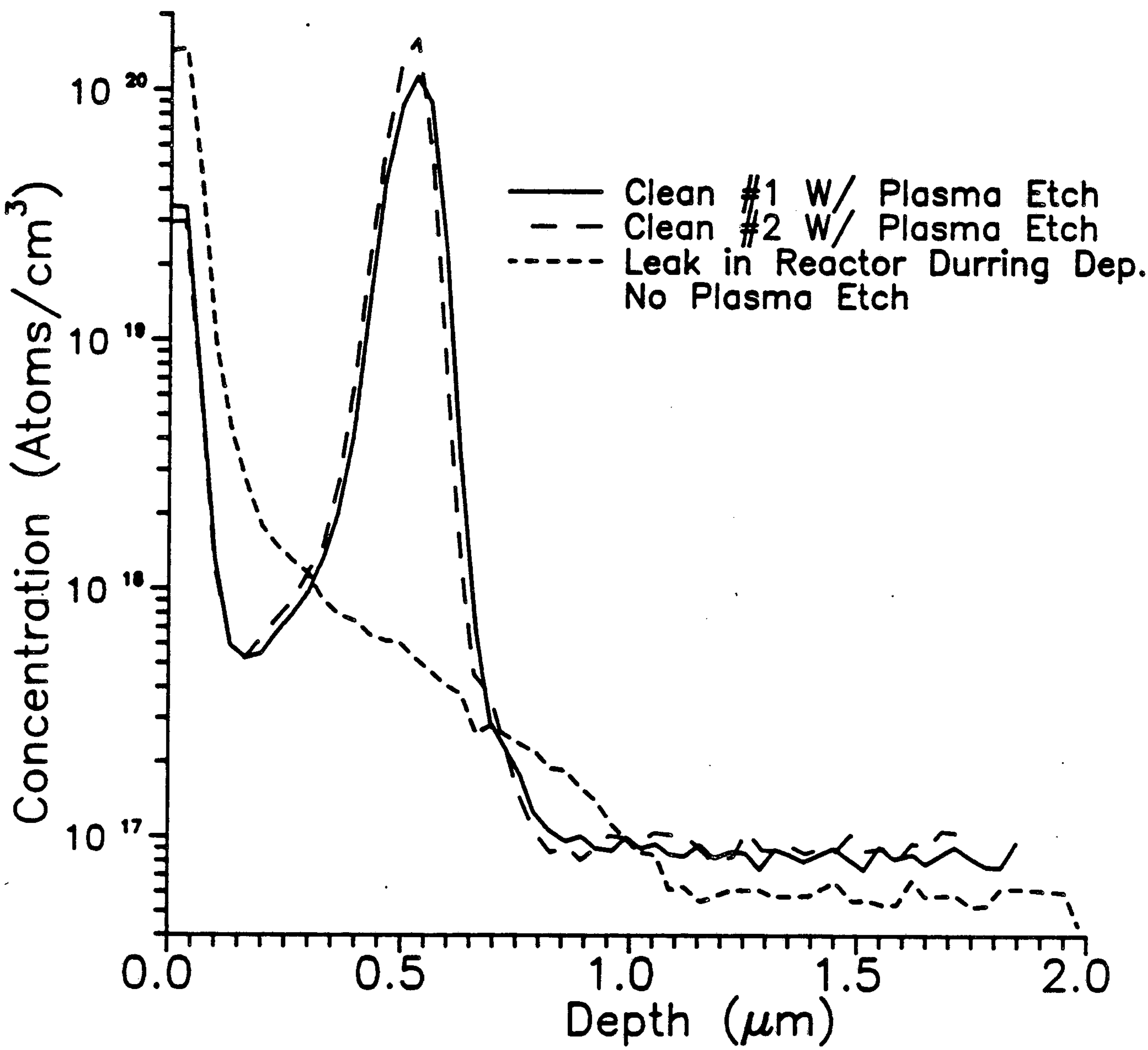

Fig. 10. SIMS of LPVPE Epi Films: Carbon Concentration

3.1.3. Preliminary detector test results

- **Responsivity**

- **Dark current**

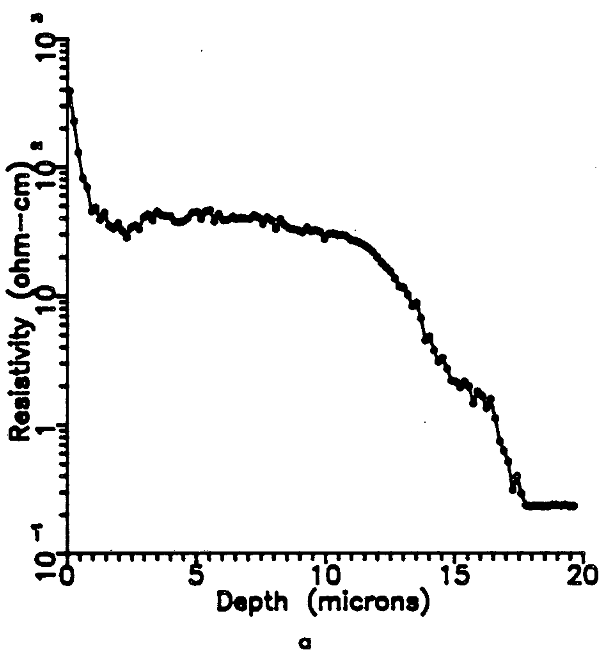

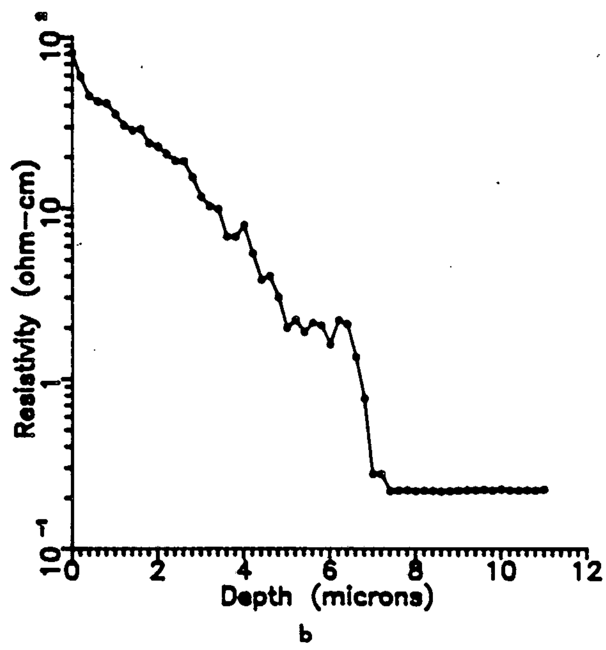

Fig. 11. Spreading resistance as a function of depth from the epilayer surface for: (a) an area of epilayer close to the leading edge of the wafer in II-16 where the growth rate was ~ 0.06 μmmin^{-1}, and (b) an area of epilayer farthest from the leading edge of the same wafer where the growth rate was ~ 0.02 μmmin^{-1}. The slight rise in resistivity at the very surface is due to the native oxide.

XBL 884-1157

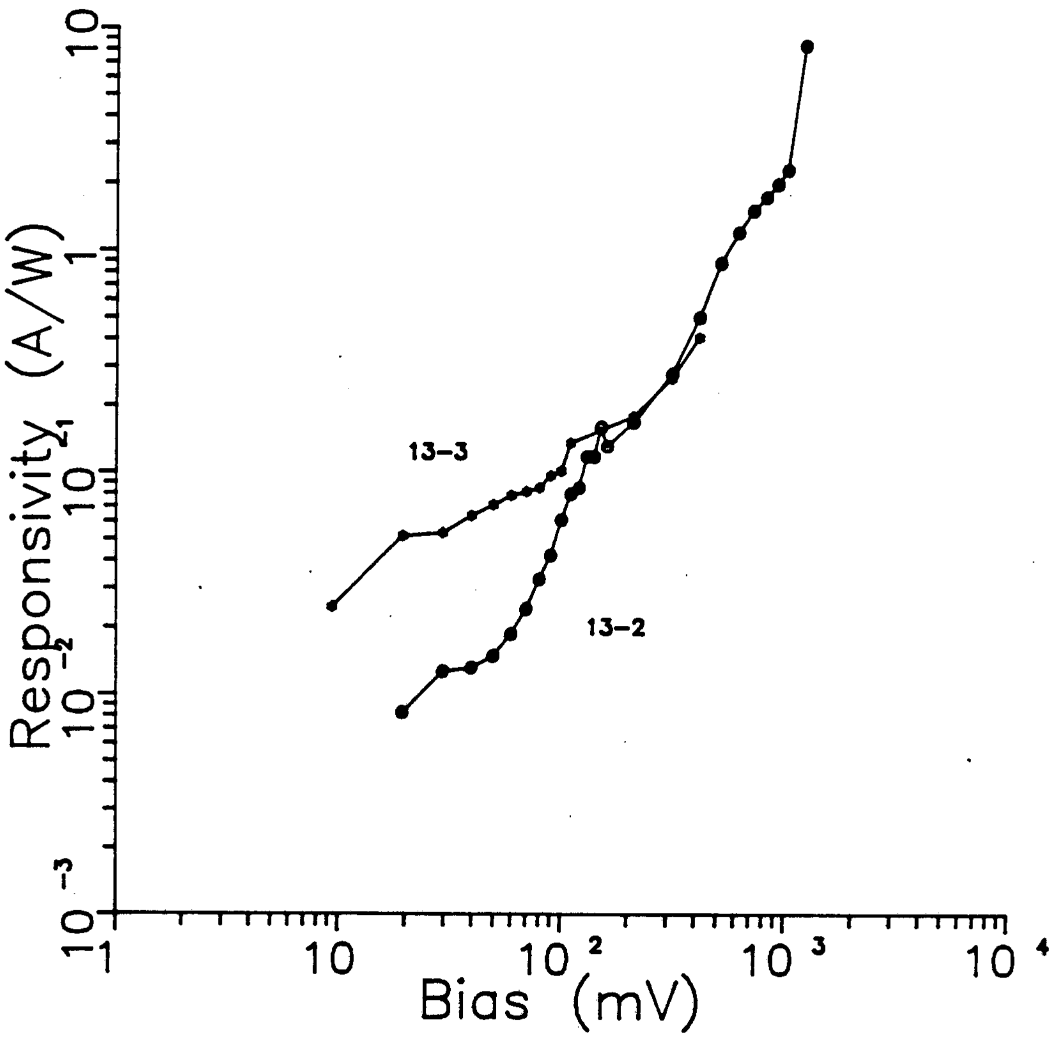

Fig. 12. Responsivity as a function of bias for detectors 13-2 and 13-3 at 2.3 K under reverse bias. The substrate material is moderately doped (5×10^{15} cm^{-3}). Such material exhibits hopping conduction but does not have extended wavelength spectral response. Tests were performed with a narrow band filter at $\lambda = 98.9$ μm.

XBL 884-1164

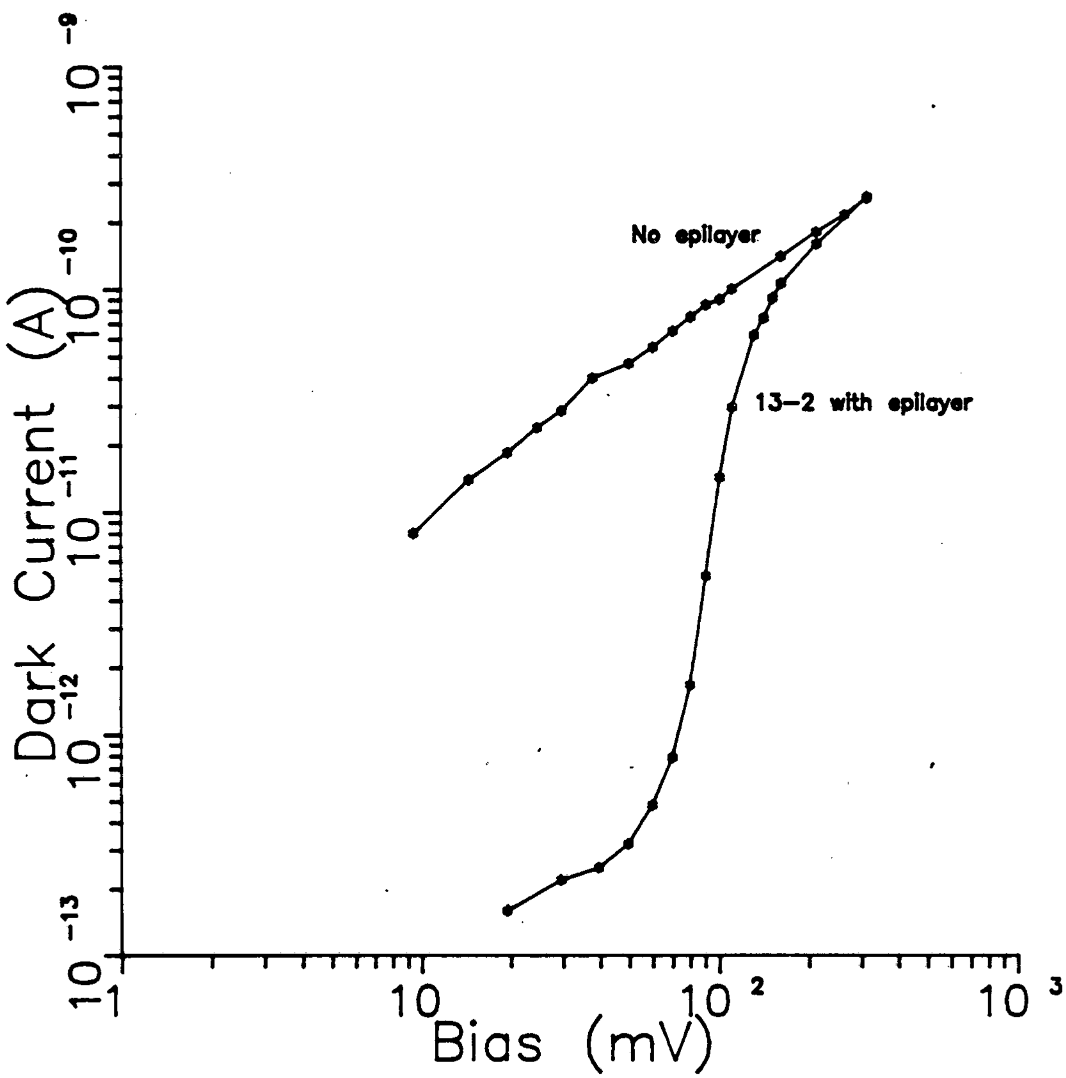

Fig. 13. Dark current as a function of detector bias for detector 13-2 with an epilayer and for the same "detector" without an epilayer at 2.3 K under reverse bias. Below a bias of ~100 mV, the blocking layer effectively reduces hopping conduction in this moderately doped material ($N_A - N_D = 5 \times 10^{15}$ cm^{-3}).

XBL 884-1160

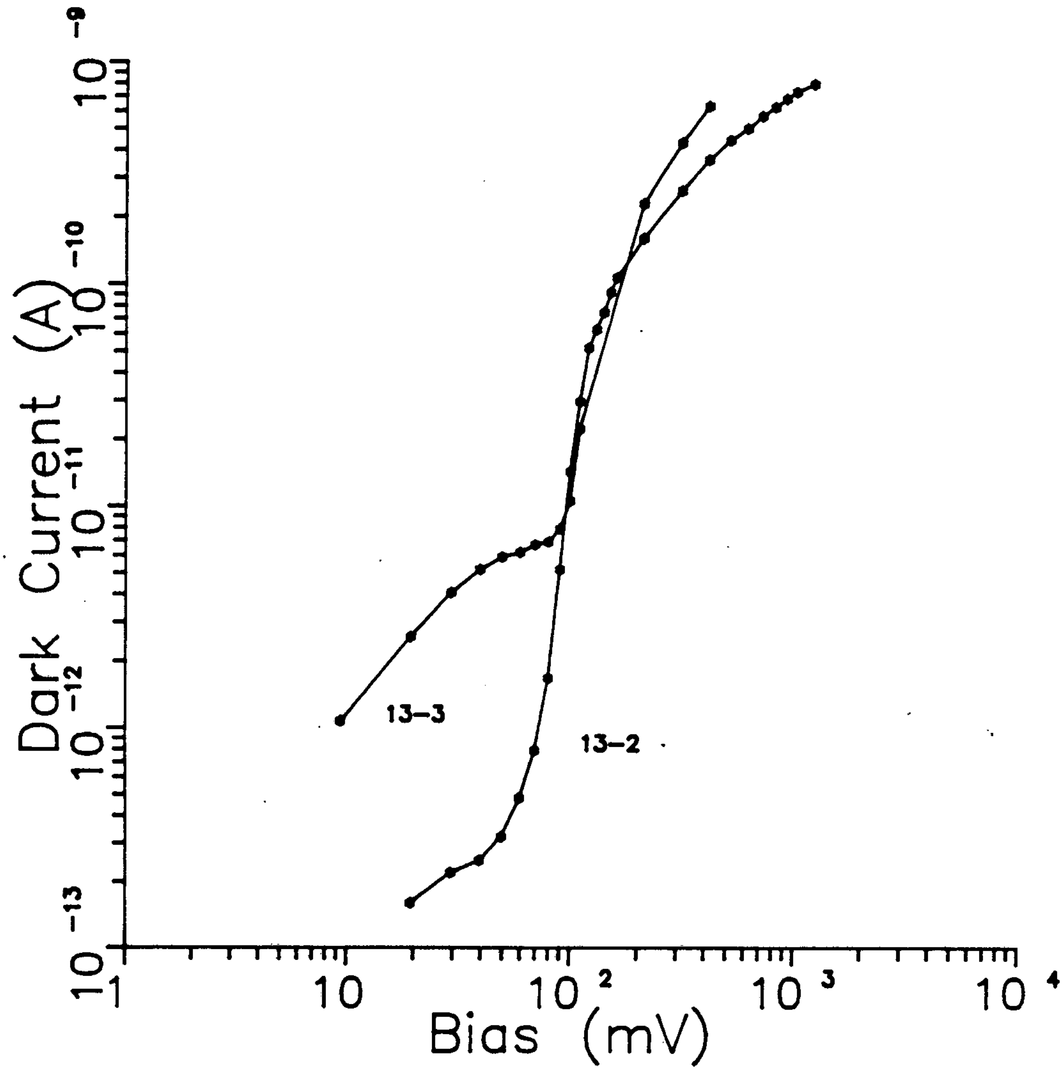

Fig. 14. Dark current as a function of bias for detectors 13-2 and 13-3 at 2.3 K under reverse bias.

XBL 884-1163

3.2. Ion Implanted BIB Detectors

- **Concept:**
  - In case pure and structurally perfect epitaxial layers are hard to produce, we can resort to implantation of dopants into an ultra-pure crystal.
- **Low energy B^+-implantation tests:**
  - three B^+ energies: 150 keV, 95 keV, 50 keV form a 0.4 μm thick layer with $N_A = 3.5 \times 10^{16}$ cm^{-3}.
  - annealing at 400°C for one hour in argon.
  - extended wavelength response.
  - responsivity = 0.5 A/W, dark current $< 10^{-14}$ A, at bias = 100 mV and T = 2.0 K. NEP $\approx 4 \times 10^{-16}$ W/ $\sqrt{\text{Hz}}$.

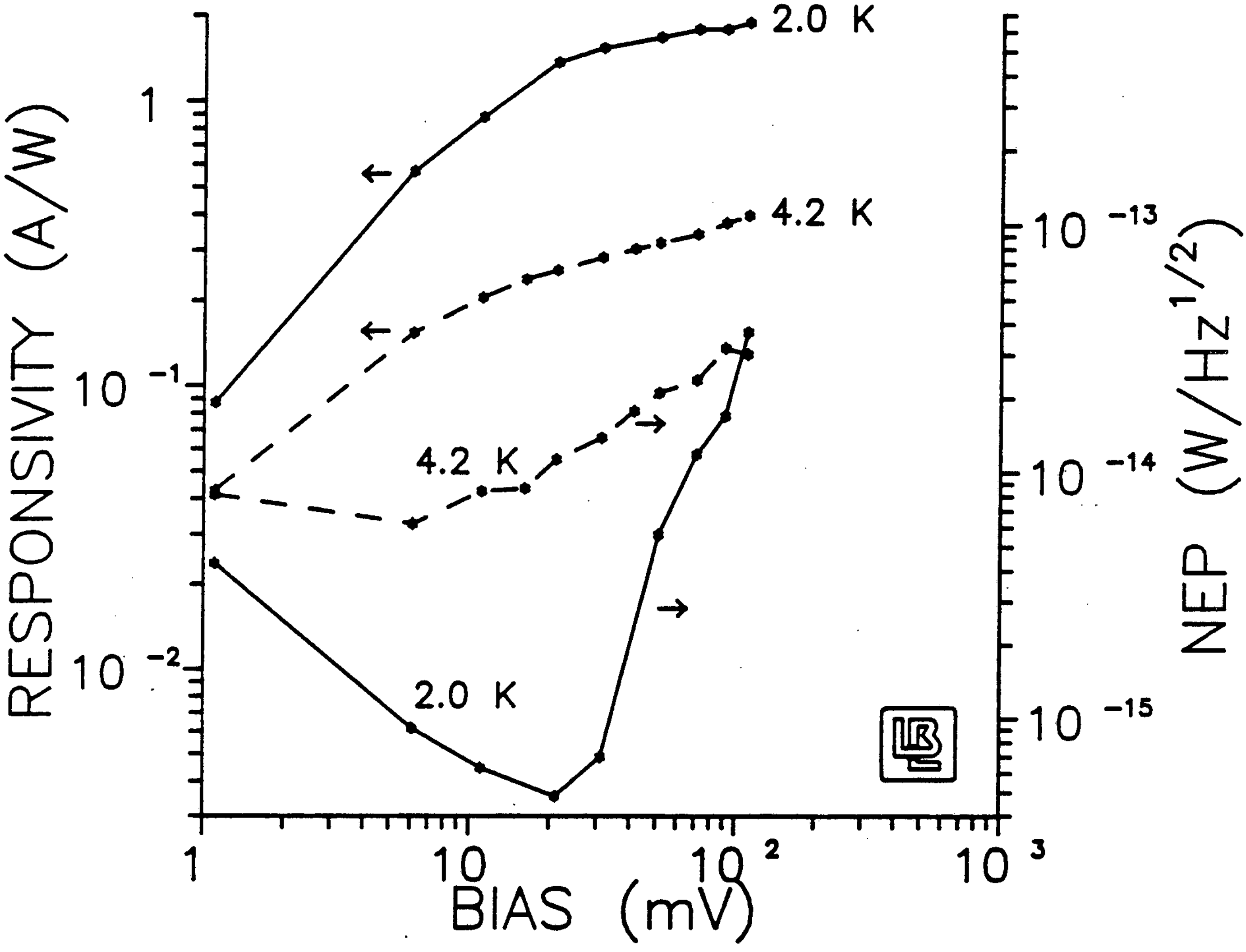

Fig. 15. Responsivity of a Ge BIB detector, low energy B^+–implant type. Active layer depth = 0.6 μm, [B] = 1 X 10^{16} cm^{-3}, λ_{filter} = 98.9 μm, $f_{chopper}$ = 23 Hz

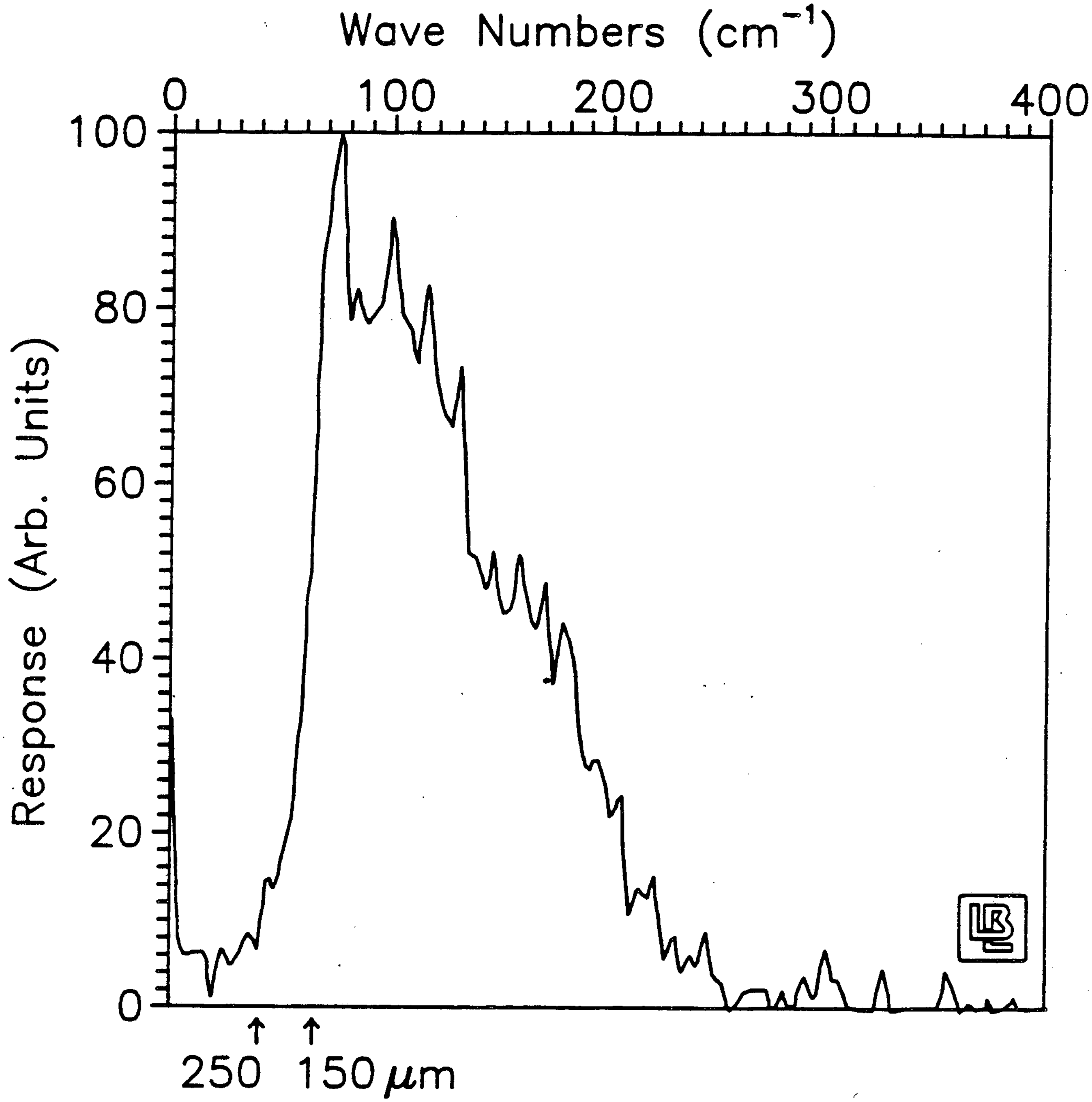

Fig. 16. Spectral response of Ge BIB detector, low energy B^+–implantation type.

- High energy B^+-implantation tests:

  - 14 implant energies up to 4 MeV doubly charged boron ions lead to a 5 μm thick layer with N_A = 1×10^{16} cm^{-3}.

  - Variable temperature Hall effect and resistivity measurements indicate full activation of shallow acceptor dopant B. No deep levels are detectable after annealing. Below 15 K, hopping conduction becomes dominant.

  - Infrared transmission measurements and device tests are in progress.

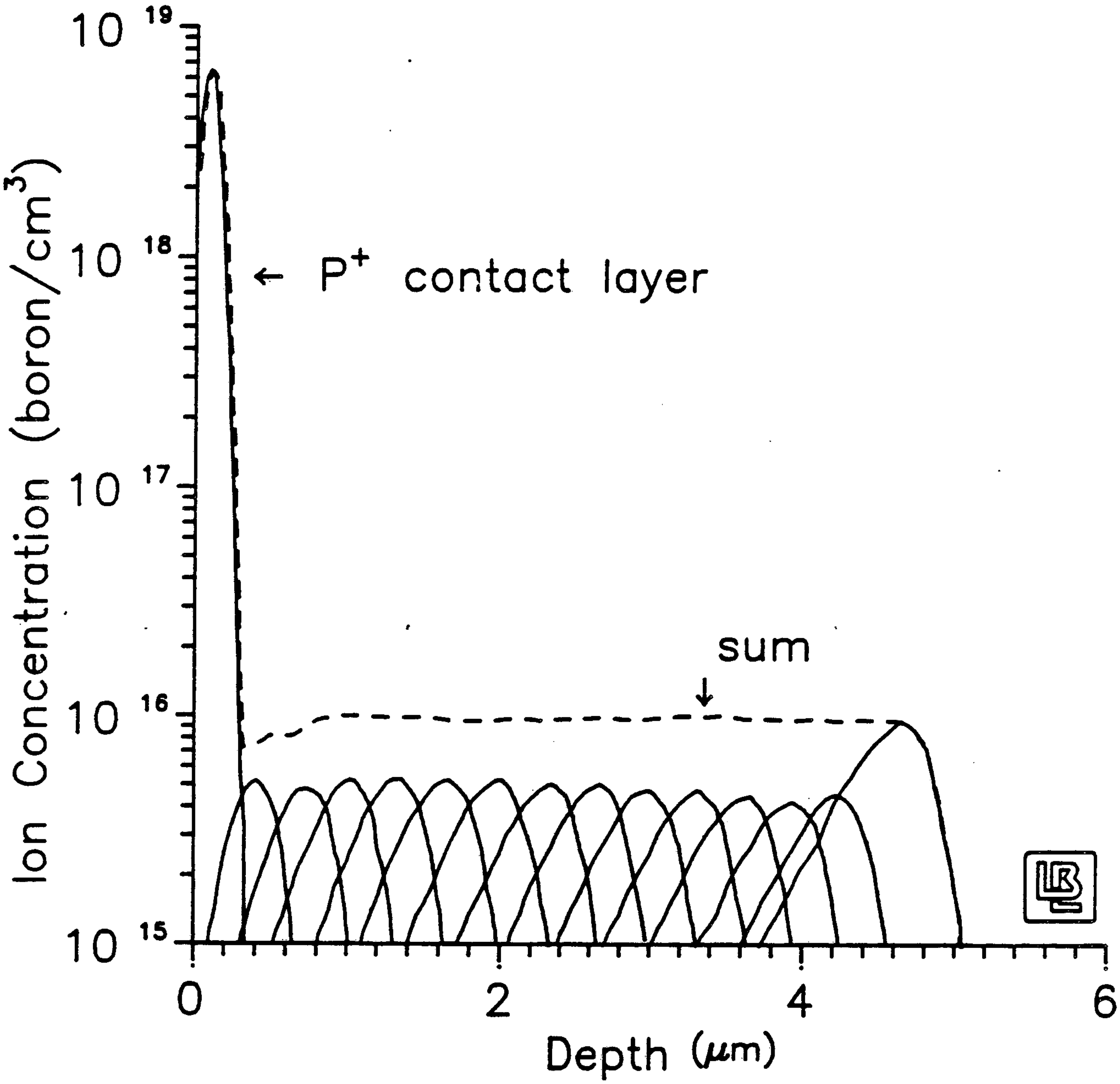

Fig. 17. Ge BIB, high energy ion implant profile

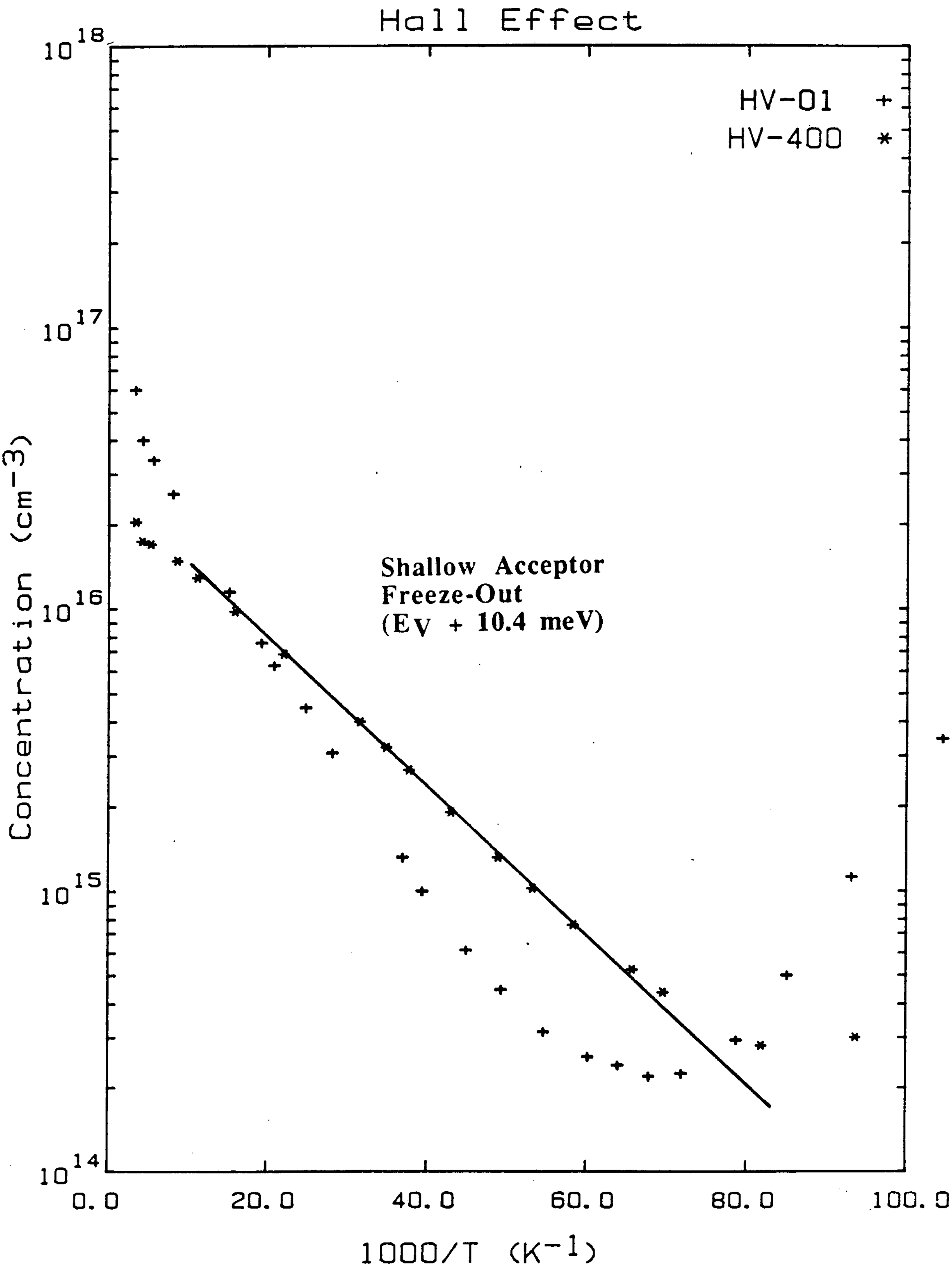

Fig. 18. Free carrier freeze-out of high energy B^+-implanted layer. Before annealing (+), the slope of the freeze-out curve is steeper than after annealing (*). The latter slope corresponds to ~ 10.4 meV, the binding energy of shallow boron acceptors. Below 15 K, hopping conduction becomes dominant.

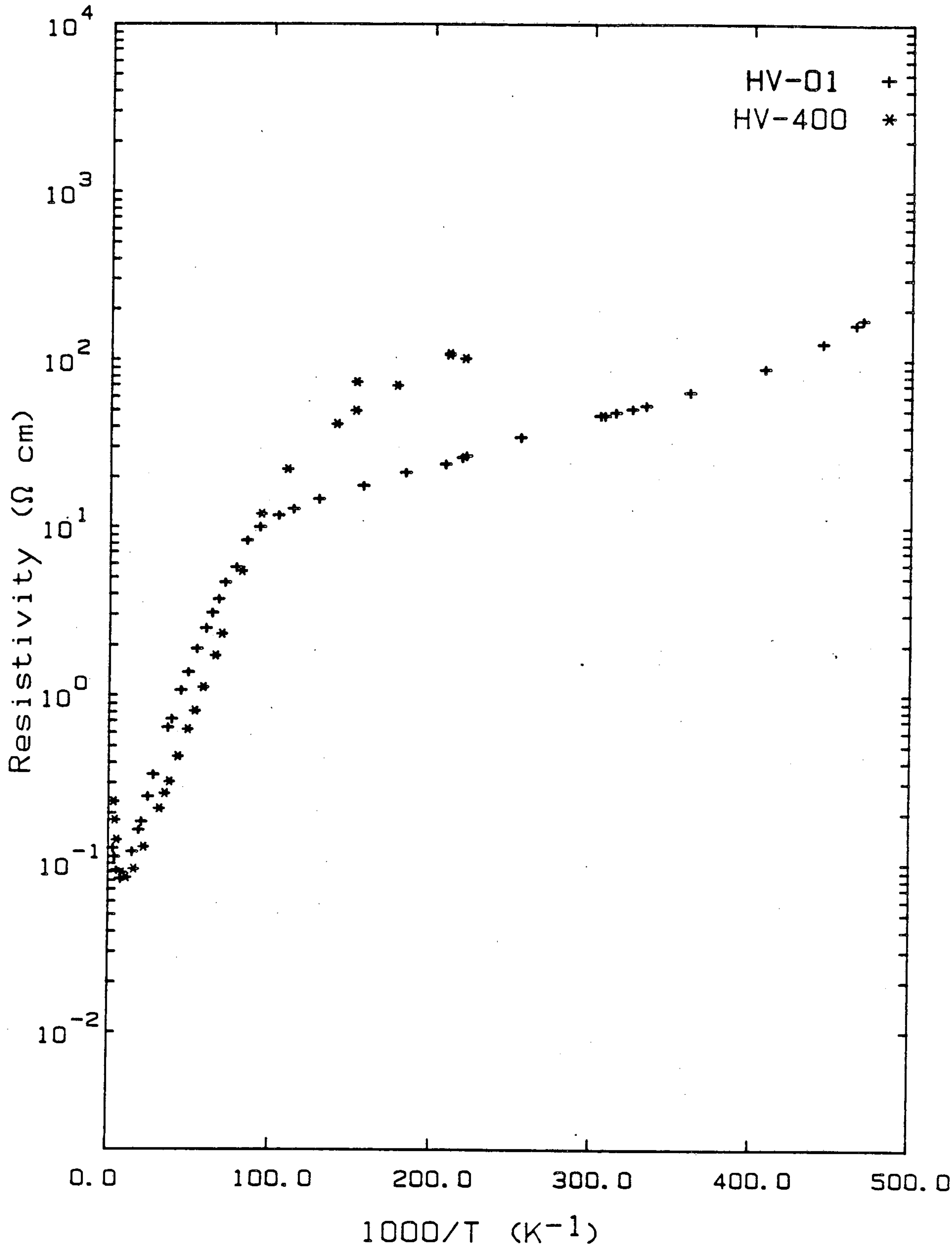

Fig. 19. Resistivity as a function of inverse temperature of the high energy B^+-implant layer before (+) and after (*) annealing. Hopping conduction becomes dominant below 15 K.

4. CONCLUSIONS

- A LPVPE technique for the low temperature growth of epitaxial Ge layers has been developed.
- Hall effect and resistivity measurements indicate that the epi layers are lightly p-type due to residual copper contamination.
- First generation Ge BIB detectors made with moderately doped substrates (5×10^{15} cm^{-3}) exhibit effective blocking of the hopping current.
- First generation Ge BIB detectors exhibit responsivities around 1 A/W.
- Second generation devices using low pressure VPE are being processed.
- Ion implanted active layers are tested.
- It is currently not known what temperatures will be required to reduce the dark current down to levels which are acceptable for SIRTF applications.

LAWRENCE BERKELEY LABORATORY
TECHNICAL INFORMATION DEPARTMENT
1 CYCLOTRON ROAD
BERKELEY, CALIFORNIA 94720